Eur. Phys. J. A **14**, 211–217 (2002)
DOI 10.1140/epja/i2001-10197-8

THE EUROPEAN PHYSICAL JOURNAL A

Polarization observables in the reaction pn → dϕ

L.P. Kaptari[a] and B. Kämpfer[b]

Forschungszentrum Rossendorf, PF 510119, 01314 Dresden, Germany

Received: 13 February 2001 / Revised version: 30 November 2001
Communicated by A. Schäfer

Abstract. The reaction $pn \to d\phi$ is studied within a covariant boson exchange model. The behavior of polarization observables being accessible in forthcoming experiments near threshold is predicted.

PACS. 13.75.-n Hadron-induced low- and intermediate-energy reactions and scattering (energy less than or equal to 10 GeV) – 14.20.-c Baryons (including antiparticles) – 21.45.+v Few-body systems

1 Introduction

Data on elementary reactions with neutrons are scarce since either they must be extracted, with some efforts and even mostly with some model-dependent assumptions, from reactions on nuclei, or a tagged neutron beam (cf. [1]) is used. The spectator technique [2,3] represents an example of how one can use a deuteron target to isolate quasi-free reactions at the neutron. It is based on the idea to measure the spectator proton ($p_{\rm sp}$) at fixed (or slightly varying) beam energy in the meson (M) production reactions $pd \to dMp_{\rm sp}$, thus exploiting the internal momentum spread of the neutron (n) inside the deuteron (d). In such a way one gets access to quasi-free reactions $pn \to dM$ if, in experiments with the deuteron target at rest, the spectator proton has momenta of the order of $50 \cdots 150$ MeV/c.

An experimental investigation of the near-threshold (pseudo)scalar and vector meson production at the neutron becomes therefore feasible. Indeed, at COSY the ANKE spectrometer set-up can be used, in particular, for studying the a_0, ω and ϕ production with the internal beam at a "neutron target" [3]. This offers the possibility to enlarge the data basis on hadronic reactions and to address special issues. For instance, there is already a large body of data which can be used for a systematic study of the OZI rule violation via ω and ϕ production in πN and pp reactions (cf. [4] for a reanalysis) and in $\bar{p}p$ annihilation (cf. [5,6] for theoretical analyses) as well. OZI rule violations are of interest with respect to possible hints to a significant $s\bar{s}$ admixture in the proton, as supported by the pion-nucleon Σ term [7,8] and interpretations of the lepton deep-inelastic scattering data [9]. Besides the impact on hadron phenomenology the origin of the OZI rule has also a link to QCD [10,11].

In the reactions $pp \to ppM$ or $pn \to pnM$ the final-state interaction among the outgoing nucleons plays a role. Therefore, the meson production process is a convolution of the "pure production process" and the final-state interaction. In the case of the reaction $pn \to dM$ one has *one* well-defined final state of the nucleons and may better constrain the elementary production amplitude.

Finally, we mention that in the reactions $pp \to ppM$, $pn \to pnM$ and $pn \to dM$ the conservation laws and symmetry principles determine a different dynamics near threshold, which needs to be investigated to allow a firm understanding of the reactions and the systematics of the OZI rule violation.

Given this motivation, in [12,13] the reaction $pn \to dV$ with $V = \omega, \phi$ has been studied in some detail. ($pn \to dS$ with $S = a_0^+, \eta, \eta'$ is considered in [14].) In [12] the cross-sections and angular distributions are elaborated as a function of the excess energy within a two-step model. The same observables are evaluated in [13] within the framework of a boson exchange model with emphasis on the ratio of cross-sections $\sigma_{pn\to d\phi}/\sigma_{pn\to d\omega}$ being of direct relevance for the OZI rule violation.

Since at COSY the proton beam is polarized and also the use of polarized targets is envisaged, we extend the previous studies [12,13] to make, for the first time, a prediction of polarization observables in the reaction $pn \to d\phi$. The set-up of the ANKE experiment at COSY can directly identify the ϕ-meson via its K^+K^- decay channel. We present the asymmetry, tensor-analyzing power, and p-ϕ spin-spin correlations. In doing so, we use our previous one-boson exchange model [15] with parameters adjusted to available near-threshold data on ϕ production in pp and πp reactions and combine this with our previous studies [15–17] employing a solution of the deuteron wave function within the Bethe-Salpeter (BS) formalism. In this

[a] On leave of absence from Bogoliubov Laboratory of Theoretical Physics, JINR, 141980 Dubna, Moscow Region, Russia.
[b] e-mail: kaempfer@fz.rassendorf.de

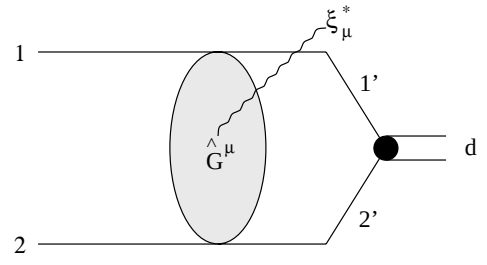

Fig. 1. The diagram for the process $p(1)+n(2)=d+\phi$. G is the scattering operator, and ξ^* denotes the polarization vector of the outgoing vector meson.

way, we derive a completely covariant approach which allows to compute the invariant amplitude $T_{NN\to\phi d}$ to be used as input into more complex processes.

Our paper is organized as follows. In sect. 2 we present the theoretical framework and elaborate the basic equations. The numerical results and their discussion are presented in sect. 3. The summary can be found in sect. 4.

2 The model

The invariant differential cross-section of the reaction $pn\to d\phi$ reads

$$\frac{\mathrm{d}\sigma}{\mathrm{d}t}=\frac{1}{16\pi\, s(s-4m^2)}\,\frac{1}{4}\sum_{s_1,s_2}\sum_{\mathcal{M}_\phi,\mathcal{M}_d}|T^{\mathcal{M}_\phi\mathcal{M}_d}_{s_1s_2}(s,t)|^2, \quad (1)$$

where s is the square of the total energy of the colliding particles p and n in the center of mass, t is the square of the transferred four-momentum from proton to deuteron, m is the nucleonic mass, $s_1, s_2, \mathcal{M}_\phi$ and $\mathcal{M}_d$ denote the spin projections on a given quantization axis, and T stands for the invariant amplitude. The general form of T may be written as (cf. fig. 1) $T^{\mathcal{M}_\phi\mathcal{M}_d}_{s_1s_2}(s,t)=\langle\, d,\mathcal{M}_d\,|\hat{G}_\mu\,\xi^{*\mu}_{\mathcal{M}_\phi}|1,2\,\rangle$, where $\xi^\mu_{\mathcal{M}_\phi}$ is the polarization four-vector of the ϕ-meson. The scattering operator $\hat{G}$ represents a four-vector in Minkowski space, and a $16\otimes 16$ component object in the spinor space of nucleons. The deuteron is described as a 16 component BS amplitude $\Phi(1,2)$ which is defined as a matrix element of a time-ordered product of two nucleon fields $\psi(x)$ by $\Phi^{\alpha\beta}(1,2)=\langle\, d|\mathcal{T}\left(\psi^\alpha(1)\psi^\beta(2)\right)|0\,\rangle$ satisfying the BS equation. By defining another scattering operator via $\hat{O}=\hat{G}_\mu\,\xi^{\mu*}_{\mathcal{M}_\phi}$ the invariant amplitude reads

$$T^{\mathcal{M}_\phi\mathcal{M}_d}_{s_1s_2}(s,t)=-i\int\frac{\mathrm{d}^4p}{(2\pi)^4}\,\bar{\Phi}^{\alpha b}_{\mathcal{M}_d}(1',2')\times\hat{O}^{bc}_{\alpha\beta}(12;1'2',\mathcal{M}_\phi)\,u^c_{s_1}(1)\,u^\beta_{s_2}(2), \quad (2)$$

where $\bar{\Phi}^{\alpha b}_{\mathcal{M}_d}(1',2')$ is the conjugate BS amplitude in the momentum space, p is the relative four-momentum of the nucleons in the deuteron, and $u(1)$ and $u(2)$ denote the Dirac spinors for the incident nucleons. Summation over spin indices $\alpha,\beta,b,c=1\cdots4$ occurring pairwise is supposed. The operator $\hat{O}^{bc}_{\alpha\beta}(12;1'2',\mathcal{M}_\phi)$ is a scattering operator describing the ϕ-meson production in the final state. This operator acts in the spinor space of protons and neutrons separately; the upper (Latin) and lower (Greek) spinor indices refer to protons and neutrons, respectively. The first indices, b and α, form an outer product of two columns, whereas the second ones, c and β, form an outer product of two rows. To specify explicitly the spinor structure we decompose the operator $\hat{O}$ in each of its indices over the corresponding complete set of Dirac spinors, *i.e.*,

$$\hat{O}^{bc}_{\alpha\beta}(12;1'2',\mathcal{M}_\phi)=\frac{1}{(2m)^4}\times\sum_{r,r',\rho,\rho'=1}^{4}A^{\mathcal{M}_\phi}_{rr',\rho\rho'}(12;1'2')u^b_{r'}(1')\bar{u}^c_r(1)\bar{u}^\beta_\rho(2)u^\alpha_{\rho'}(2'), \quad (3)$$

where the coefficients $A^{\mathcal{M}_\phi}_{rr',\rho\rho'}(12;1'2')$ may be found by using the completeness and orthogonality of the Dirac spinors, $\bar{u}_r(\boldsymbol{p})u_{r'}(\boldsymbol{p})=2\varepsilon_r m\delta_{rr'}$, yielding

$$A^{\mathcal{M}_\phi}_{rr',\rho\rho'}(12;1'2')=\varepsilon_r\varepsilon_{r'}\varepsilon_\rho\varepsilon_{\rho'}\,\bar{u}^b_{r'}(1')\,\bar{u}^\alpha_{\rho'}(2')\times\hat{O}^{bc}_{\alpha\beta}(12;1'2',\mathcal{M}_\phi)\,u^c_r(1)\,u^\beta_\rho(2), \quad (4)$$

where $\varepsilon_r=+1$ for $r=1,2$ and $\varepsilon_r=-1$ for $r=3,4$. Substituting (3) into (2) one obtains

$$\begin{aligned}T^{\mathcal{M}_\phi\mathcal{M}_d}_{s_1s_2}(s,t)&=\frac{-i}{(2m)^2}\int\frac{\mathrm{d}^4p}{(2\pi)^2}\bar{\Phi}^{\alpha b}_{\mathcal{M}_d}(1',2')\\&\times\sum_{r,r'=1}^{2}A^{\mathcal{M}_\phi}_{s_1s_2,rr'}(12;1'2')\,u^\alpha_{r'}(2')u^b_r(1')=\\&\frac{i}{(2m)^2}\sum_{r,r'=1}^{2}\int\frac{\mathrm{d}^4p}{(2\pi)^2}\left(u^\alpha_{r'}(2')\right)^T\gamma_{\mathrm{c}}^{\alpha\alpha'}\\&\times\left(\gamma_{\mathrm{c}}^{\alpha'\alpha''}\bar{\Phi}^{\alpha''b}_{\mathcal{M}_d}(1',2')\right)A^{\mathcal{M}_\phi}_{s_1s_2,rr'}(12;1'2')u^b_r(1')=\\&\frac{i}{(2m)^2}\sum_{r,r'=1}^{2}\int\frac{\mathrm{d}^4p}{(2\pi)^4}A^{\mathcal{M}_\phi}_{s_1s_2,rr'}(12;1'2')\\&\times\bar{v}_{r'}(2')\,\bar{\Psi}_{\mathcal{M}_d}(1',2')\,u_r(1'),\end{aligned} \quad (5)$$

where γ_{c} is the charge conjugation matrix, $\bar{v}_r(2')\equiv(u_r(2'))^T\gamma_{\mathrm{c}}$, and the new BS amplitude $\bar{\Psi}_{\mathcal{M}_d}(1',2')\equiv\gamma_{\mathrm{c}}\bar{\Phi}_{\mathcal{M}_d}(1',2')$ now is a $4\otimes4$ matrix and represents the solution of the BS equation written also in matrix form. Note that in eq. (5), contrary to eq. (3), the summation over the indices r,r' is restricted to two values. The reason is the following: In the matrix form, the partial BS amplitudes explicitly contain projection operators onto either positive- or negative-energy states [17] which select from eq. (3) $r,r'=1,2$ or $r,r'=3,4$. The main contribution to the considered near-threshold process comes from the positive-energy partial amplitudes S^{++} and D^{++}. The other six amplitudes have been neglected in the present work due to their smallness within the near-threshold kinematics (see, *e.g.* [17]). Then from the explicit expression of the S^{++} and D^{++} components [17] (cf. eq. (6) below) one has in eq. (5) $r,r'=1,2$.

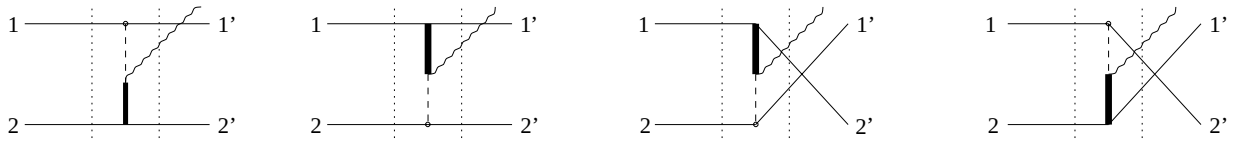

Fig. 2. Graphical representation of the operator $\hat{O}$ defined in (3) in the one-boson exchange approximation. Nucleons in the initial and final states are represented by thin lines which are truncated by vertical dotted lines as to obtain an operator. The exchanged π- and ρ-mesons are depicted by vertical dashed and thick lines, respectively. The four different contributions correspond to different combinations of $\pi^0, \pi^\pm$ and $\rho^0, \rho^\pm$ exchanges.

For further evaluations of the amplitude (5) one needs to specify an explicit form of the operator $\hat{O}$. By sandwiching the operator $\hat{O}$ in eq. (3) between two-nucleon states (on-shell nucleons) one gets the amplitude $A^{\mathcal{M}_\phi}_{rr',\rho\rho'}(12;1'2')$ of real processes of ϕ-meson production in NN reactions. That means $\hat{O}$ can be constructed from two parts: i) a part which coincides formally with the free NN operator, however, with effective couplings which, in general, can differ from the on-shell fixings and ii) other additional off-shell terms vanishing, as the corresponding matrix elements, in free NN scattering. Near the threshold one may expect that the off-mass shell part plays a minor role and in what follows it can be neglected. Moreover, in this region the effective constants (cut-off, couplings, etc.) may be safely taken as in the free case. Then the operator $\hat{O}$ follows from an effective meson-nucleon theory with interaction Lagrangians for the πNN, ρNN, $\phi\rho\pi$ vertices by calculating the relevant truncated Feynman diagrams with a ϕ-meson in the final state. In terms of strict one-boson exchange contributions, the Feynman diagrams can be grouped into two classes: the meson exchange diagram with internal meson conversion and diagrams with direct emission of the ϕ-meson from a nucleonic line, the nucleonic current diagrams. In refs. [13,15] parameter sets have been found where the contributions from the nucleonic currents are negligibly small for the free $NN \to NN\phi$ processes. As a result, in the reaction $pn \to d\phi$ such diagrams with nucleonic current emission can be omitted as well, when using the corresponding parameter sets. Then we are left with the exchange process with internal meson conversion, and $\hat{O}$ can be represented by the four truncated diagrams as depicted in fig. 2 with effective parameters taken, *e.g.*, from [13,15]. Hence, having computed these diagrams it is straightforward to obtain the coefficients $A^{\mathcal{M}_\phi}_{rr',\rho\rho'}(12;1'2')$ in (4). It is worth stressing here that, if all particles were on mass shell, $A^{\mathcal{M}_\phi}_{rr',\rho\rho'}(12;1'2')$ exactly coincides with the amplitude of the elementary free process $1+2 \to 1'+2'+\phi$. However, in our case this amplitude corresponds to a virtual subprocess of vector meson production with two off-shell nucleons in the final state. The off-shellness of the final nucleons is consistently taken into account by solving the full spinor-spinor Bethe-Salpeter equation for the deuteron with a realistic one-boson exchange kernel with both nucleons off-mass shell.

Since our numerical solution [18] of the BS equation has been obtained in the deuteron's center of mass, all further calculations will be performed in this system. First, as depicted in fig. 1, we introduce the relevant kinematical variables as follows: $p_{1,2}$ are the four-momenta of incoming nucleons, $p'_{1,2}$ stand for the four-momenta of the internal (off-shell) nucleons in the deuteron with $p = (p'_1 - p'_2)/2$; $\xi_{\mathcal{M}_d}$ denotes the polarization four-vector of the deuteron. In this notation the S^{++} and D^{++} partial BS amplitudes in the deuteron's rest system are of the form [17]

$$\Psi^{S^{++}}_{\mathcal{M}_d}(p'_1,p'_2) = \mathcal{N}(\hat{k}_1+m)\frac{1+\gamma_0}{2}\hat{\xi}_{\mathcal{M}_d}(\hat{k}_2-m)\phi_S(p_0,|\boldsymbol{p}|),$$

$$\Psi^{D^{++}}_{\mathcal{M}_d}(p'_1,p'_2) = -\frac{\mathcal{N}}{\sqrt{2}}(\hat{k}_1+m)\frac{1+\gamma_0}{2}$$
$$\times\left(\hat{\xi}_{\mathcal{M}_d}+\frac{3}{2|\boldsymbol{p}|^2}(\hat{k}_1-\hat{k}_2)(p\xi_M)\right)(\hat{k}_2-m)\phi_D(p_0,|\boldsymbol{p}|), \quad (6)$$

where "$\hat{}$" means contraction with Dirac matrices, and $k_{1,2}$ are on-shell four-vectors related to the off-shell vectors $p'_{1,2}$ as follows:

$$k_1 = (E_p,\boldsymbol{p}), \quad k_2 = (E_p,-\boldsymbol{p}),$$
$$p'_1 = (p'_{10},\boldsymbol{p}), \quad p'_2 = (p'_{20},-\boldsymbol{p}), \quad E_p = \sqrt{\boldsymbol{p}^2+m^2}, \quad (7)$$

and $\phi_{S,D}(p_0,|\boldsymbol{p}|)$ are the partial scalar amplitudes related to the corresponding partial vertices as

$$\phi_{S,D}(p_0,|\boldsymbol{p}|) = \frac{G_{S,D}(p_0,|\boldsymbol{p}|)}{\left(\frac{1}{2}M_d - E_p\right)^2 - p_0^2}. \quad (8)$$

M_d is the deuteron mass, and the normalization factor is $\mathcal{N} = \left\{\sqrt{8\pi}2E(E+m)\right\}^{-1}$. To be explicit let us recall the components of the polarization four-vector of a vector particle with four-momentum $p = (E,\boldsymbol{p})$, polarization index $\mathcal{M} = \pm1, 0$ and mass M as

$$\xi_{\mathcal{M}} = \left(\frac{\boldsymbol{p}\boldsymbol{\xi}_{\mathcal{M}}}{M}, \boldsymbol{\xi}_{\mathcal{M}} + \boldsymbol{p}\frac{\boldsymbol{p}\boldsymbol{\xi}_{\mathcal{M}}}{M(E+M)}\right), \quad (9)$$

where $\boldsymbol{\xi}_{\mathcal{M}}$ is the polarization three-vector for the particle at rest with $\boldsymbol{\xi}_{+1} = -\frac{1}{\sqrt{2}}(1,i,0)$, $\boldsymbol{\xi}_{-1} = \frac{1}{\sqrt{2}}(1,-i,0)$, $\boldsymbol{\xi}_0 = (0,0,1)$. The above Dirac spinors, normalized as $\bar{u}(p)u(p) = 2m$ and $\bar{v}(p)v(p) = -2m$, read

$$u(\boldsymbol{p},s) = \sqrt{m+\epsilon}\begin{pmatrix}\chi_s\\ \frac{\boldsymbol{\sigma p}}{m+\epsilon}\chi_s\end{pmatrix},$$

$$v(\boldsymbol{p}\,,s) = \sqrt{m+\epsilon}\begin{pmatrix}\frac{\boldsymbol{\sigma p}}{m+\epsilon}\widetilde{\chi}_s\\ \widetilde{\chi}_s\end{pmatrix}, \quad (10)$$

where $\widetilde{\chi}_s \equiv -i\sigma_y\chi_s$, and χ_s denotes the usual two-dimensional Pauli spinor. In general, the BS amplitude consists of eight partial components. In eqs. (5), (6) we take into account only the most important ones, namely the S and D partial amplitudes. The other six amplitudes might become important only at high transferred momenta [16,17], hence for the present near-threshold process they may be safely disregarded. Therefore, $r, r' = 1, 2$, as already mentioned above. Substituting eqs. (6)-(10) into (5) one obtains after some algebra

$$
\begin{aligned}
&T^{\mathcal{M}_\phi\mathcal{M}_d}_{s_1s_2}(s,t) = \\
&\frac{-i}{\sqrt{8\pi}}\sqrt{|\mathcal{M}_d|+1}\sum_{r,r'=1}^{2}\int\frac{\mathrm{d}^4p}{2E_p(2\pi)^4}\frac{G_S - G_D\frac{1}{\sqrt{2}}}{\left(\frac{1}{2}M_d - E_p\right)^2 - p_0^2} \\
&\times A^{\mathcal{M}_\phi}_{s_1s_2,rr'}(\boldsymbol{p}_1\boldsymbol{p}_2,\boldsymbol{p}_1'\boldsymbol{p}_2')\,\delta_{r+r',\mathcal{M}_d} \\
&+\frac{3i}{\sqrt{16\pi}}\sum_{r,r'=1}^{2}\int\frac{\mathrm{d}^4p}{2E_p(2\pi)^4}\frac{G_D}{\left(\frac{1}{2}M_d - E_p\right)^2 - p_0^2} \\
&\times A^{\mathcal{M}_\phi}_{s_1s_2,rr'}(\boldsymbol{p}_1\boldsymbol{p}_2,\boldsymbol{p}_1'\boldsymbol{p}_2')\widetilde{\chi}^+_{r'}\,(\boldsymbol{\sigma n})\chi_r\,(\boldsymbol{n}\boldsymbol{\xi}^*_{\mathcal{M}_d})\,. \qquad (11)
\end{aligned}
$$

By closing the integration contour in the upper hemisphere and picking up the residuum at $p_0 = M_d/2 - E_p$ and introducing the notion of the deuteron S and D wave functions as

$$
\begin{aligned}
u_S(p) &= \frac{G_S(p_0,|\boldsymbol{p}|)}{4\pi\sqrt{2M_d}(2E_p - M_d)}, \\
u_D(p) &= \frac{G_D(p_0,|\boldsymbol{p}|)}{4\pi\sqrt{2M_d}(2E_p - M_d)} \qquad (12)
\end{aligned}
$$

with $2\int \mathrm{d}\,|\boldsymbol{p}|\,|\boldsymbol{p}|^2(u_S^2 + u_D^2) \approx \pi$, the final expression for the amplitude may be written as

$$
\begin{aligned}
&T^{\mathcal{M}_\phi\mathcal{M}_d}_{s_1s_2}(s,t) = \\
&\sqrt{\frac{M_d}{4\pi}}\sum_{r,r'=1}^{2}\int\frac{\mathrm{d}^3\boldsymbol{p}}{E_p(2\pi)^2}A^{\mathcal{M}_\phi}_{s_1s_2,rr'}(\boldsymbol{p}_1,\boldsymbol{p}_2;\boldsymbol{p},-\boldsymbol{p}) \\
&\times\Bigg\{\sqrt{|\mathcal{M}_d|+1}\left[u_S(p) - \frac{u_D(p)}{\sqrt{2}}\right]\delta_{r+r',\mathcal{M}_d} \\
&-3\frac{u_D(p)}{\sqrt{2}}\left(\boldsymbol{\xi}^*_{\mathcal{M}_d}\boldsymbol{n}\right)\,\widetilde{\chi}^+_{r'}(\boldsymbol{\sigma n})\chi_r\Bigg\}, \qquad (13)
\end{aligned}
$$

where $\boldsymbol{n}$ is a unit vector parallel to $\boldsymbol{p}$. The amplitude eq. (13) has been obtained in the deuteron center-of-mass system, hence it is not manifestly covariant. However, since the transformation properties of the BS amplitude under Lorentz-boosts are well known (see, *e.g.* [17]) this amplitude may be written in any frame of reference. In the chosen system it has the simplest form. Moreover, in this system a direct non-relativistic treatment of the obtained formulae becomes straightforward. Indeed, the above introduced BS wave functions $u_{S,D}(p)$ are directly related to the non-relativistic deuteron wave functions $u_L^{\mathrm{NR}}(p) = \int u_L^{\mathrm{NR}}(r)j_L(pr)r\mathrm{d}r$, where $u_L^{\mathrm{NR}}(r)$, $L = 0, 2$ are the usual S and D components of the deuteron wave function obtained within a realistic NN potential approach; for small values of the internal momentum p the BS and non-relativistic wave functions practically coincide [17]. Now, by observing that $\sqrt{2}\sum\langle\frac{1}{2}\nu_1\,\frac{1}{2}\nu_2\,|1\mathcal{M}_d\rangle\,\chi_{\frac{1}{2}\nu_1}\chi^T_{\frac{1}{2}\nu_2} = i(\boldsymbol{\sigma}\boldsymbol{\xi}_{\mathcal{M}_d})\sigma_y$ and $\delta_{r+r',\mathcal{M}_d}\sqrt{|\mathcal{M}_d|+1} = \sqrt{2}\sum\langle\frac{1}{2}r_1\,\frac{1}{2}r_2\,|1\mathcal{M}_d\rangle$, where the sums run over $\nu_{1,2} = \pm\frac{1}{2}$, and recalling that in our notation $\widetilde{\chi}_s = -i\sigma_y\chi_s$ the non-relativistic correspondence of eq. (13) becomes transparent: Since the spin structures of matrix elements are identical in the relativistic and non-relativistic cases, and due to the similarity of the corresponding wave functions, eq. (13) in the deuteron's center-of-mass system has the same form for both the relativistic and non-relativistic approaches. Nevertheless, as seen from eq. (13) even near the threshold, moderate and relatively high internal momenta p contribute to the integral, and the numerical results for observables may depend upon details of the deuteron wave function computed within different approaches. In particular, this might concern the S-wave, which is known to differ within different approaches, (*e.g.*, crossing the p-axis, where it changes the sign, or the contribution of negative parts etc.; cf. [17] and further references therein).

In what follows we compare results obtained with our BS solution [18] with non-relativistic calculations relying on Bonn and Paris wave functions. Note that the integral over p in eq. (13) formally is extended up to infinity. It is clear that, since the internal momenta of the deuteron in eq. (13) is also connected with the amplitude of processes with the ϕ-meson and virtual nucleons in the final state, the values of p corresponding to imaginary masses must be suppressed. We do so by constraining the upper limit of the p integration to $p_{\max} = 3m/4$.

3 Discussion of results

In our evaluation of the above equations we use, for describing the deuteron wave function, our numerical solution of the BS equation [18] in ladder approximation obtained with a realistic one-boson exchange interaction which includes $\pi, \sigma, \omega, \delta, \rho$ and η exchanges. The effective parameters used in the ladder approximation have been fixed in such a way to obtain a good description of the NN elastic scattering data and the static properties of the deuteron [17]. Independent of this set of parameters related to deuteron properties, the effective coupling constants and the attributed cut-off factors are taken from the recent analysis [15]. In all subsequent numerical calculations the set B from [15] is used. For this parameter set the meson exchange term is by far dominating.

In fig. 3 the total cross-section near the threshold is depicted. The full curve corresponds to our fully relativistic calculations whereas the dashed (dotted) curve represents results of non-relativistic calculations with Bonn (Paris) wave functions. It is seen that the relativistic results are quite similar to those obtained with the Paris wave function but differ by more than 50% from the ones

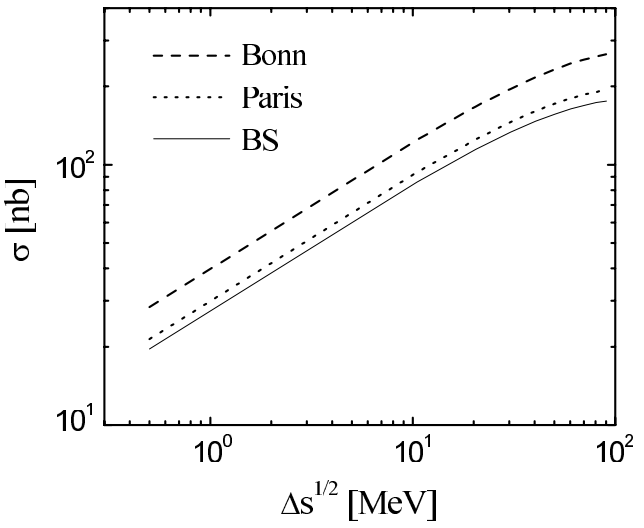

Fig. 3. Total cross-section for the reaction $pn \to d\phi$ as a function of the excess energy $\Delta s^{1/2} = \sqrt{s} - M_d - M_\phi$.

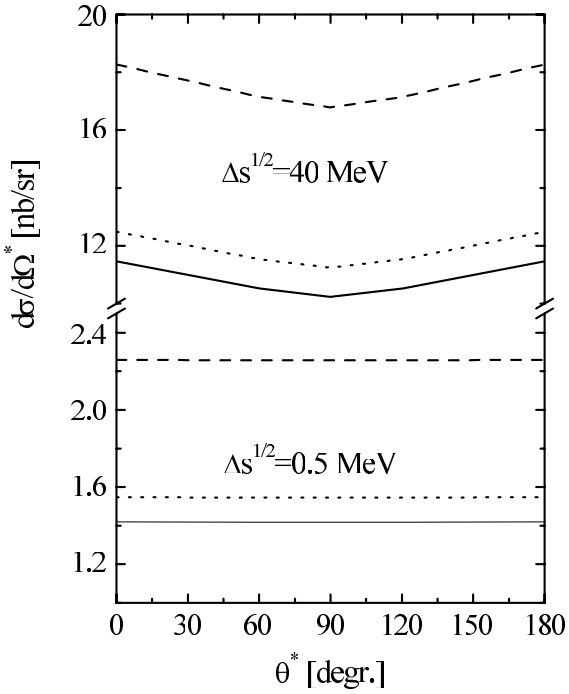

Fig. 4. Angular distribution in the center-of-mass system for two values of the excess energy. Lines as in fig. 3.

obtained within Bonn potential. This is a direct consequence of the different behavior of the S- and D-waves in the deuteron with BS and Bonn and Paris potentials. Remind that BS and Paris wave functions are essentially the same in a large interval of p, up to $p \approx 1$ GeV/c [17], whereas the Bonn wave function exhibits a different shape already at $p \geq 0.3$ GeV/c. In particular, at $p \geq 0.4$ GeV/c the contribution of the BS and Paris S-waves to the integral (13) becomes negative and quite large, whereas for the Bonn wave function the negative contribution starts at $p \sim 0.5$ GeV/c and is smaller in comparison with, *e.g.*, the Paris wave function. The shape of our cross-section is rather similar to the one computed in [13]. However, there is a difference in the absolute values by roughly 60% for BS results and 15–20% for the Bonn potential. The first difference is in the same order of magnitude as the difference of the previously often used cross-section $\sigma = 0.26$ μb deduced from [19] and the published value $\sigma = 0.19$ μb [20] for the reaction $pp \to pp\phi$ at an excess energy of 83 MeV.

References [13,15] show that several sets of parameters equally well describe the $pp \to pp\phi$ data. These sets differ not only by absolute values of parameters but also by the relative contributions of meson current and the nucleon current terms. Since in case of the $pn \to d\phi$ processes the isospin transition corresponds to $\Delta I = 0$ the meson exchange diagrams are enhanced by a factor of three in comparison with the nucleon current terms. This means that i) the contributions of the nucleon current are suppressed by about one order of magnitude in comparison with the meson current, and ii) the behavior of the cross-section and angular distribution in the process $pn \to d\phi$ is expected to follow essentially the behavior of the dominating meson exchange current contribution in the elementary processes $pn \to pn\phi$. The occurrence of the deuteron wave function only modifies this behavior. This is clearly seen in fig. 4, where the shape of the angular distribution is very similar to the distribution found in [15] for the reaction $pn \to pn\phi$. At the threshold the distribution is fairly flat, while with increasing excess energy some forward-backward peaking becomes visible. This feature depends upon the parameter set used. For instance, if we were using the set C of [15], then a slight suppression of the cross-section would be expected in the forward-backward directions as predicted for the elementary cross-section [15]. This sensitivity of the predicted angular distribution has been pointed out in [13,21] as a tool to constrain further the parameters, if precise data become available.

Let us now discuss the polarization observables. Near the threshold, in the final state the relative $\phi - d$ orbital momentum is zero and one has $I_\mathrm{f} = 0$, $J^\pi_d = 1^+$ ($L_d = 0, 2$), $J^\pi_\mathrm{f} = J^\pi_\phi + J^\pi_d = 0^-, 1^-, 2^-$, where I, L, J and π are the total isospin, total radial angular momentum, angular momentum and parity, respectively. Thus from symmetry constraints, in the initial state the allowed configurations are $I_\mathrm{i} = 0$, $L_\mathrm{i} = 1, 3, 5 \cdots$ and total spin $S_\mathrm{i} = 0$. The conservation law ($J_\mathrm{i} = J_\mathrm{f}$) implies $L_\mathrm{i} = 1$, so that $J^\pi_\mathrm{i} = 1^-$. Since $\Delta S = 1$ and $S_\mathrm{i} = 0$ after a spin-flip transition the most probable deuteron projections are expected to be $\mathcal{M}_d = \pm 1$, and consequently for the ϕ-meson $\mathcal{M}_\phi = \mp 1$ provided the S-wave in the deuteron dominates near the threshold. From these transitions in $|T^{\mathcal{M}_\phi \mathcal{M}_d}_{s_1 s_2}(s,t)|^2$ one may form different combinations of spin observables, which near the threshold behave quite differently. If one considers, for example, the cross-section averaged over all final projections $\mathcal{M}$ at different initial-spin projections, then the beam target asymmetry, defined here as

$$\mathcal{A} = \frac{\sigma(s_p{+}s_n = 1) + \sigma(s_p{+}s_n = -1) - \sigma(s_p{+}s_n = 0)}{\sigma(s_p{+}s_n = 1) + \sigma(s_p{+}s_n = -1) + \sigma(s_p{+}s_n = 0)}, \tag{14}$$

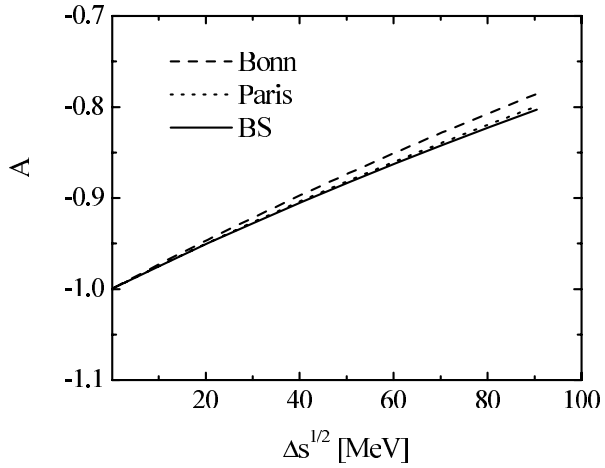

Fig. 5. The beam target asymmetry $\mathcal{A}$ as a function of the the excess energy.

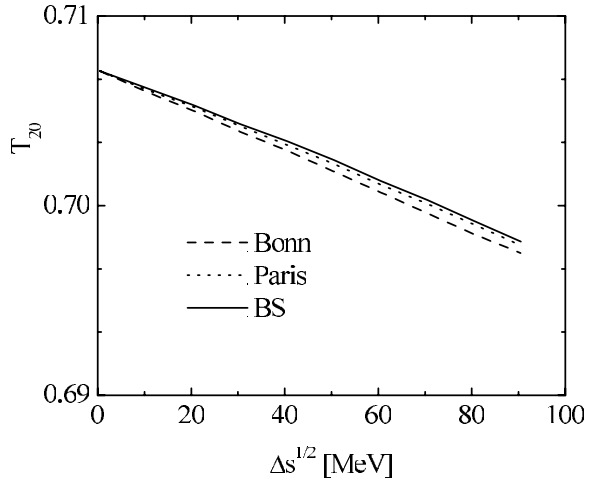

Fig. 6. Deuteron tensor-analyzing power T_{20} as a function of the excess energy.

is predicted to be -1 near threshold and to increase with increasing energy. This is in contrast with the asymmetry defined for the elementary process $pp \to pp\phi$ which is $+1$, as predicted in [15], and decreases with increasing energy. The energy dependence of the asymmetry (14) is depicted in fig. 5.

Another interesting polarization observable is the tensor-analyzing power, which may be defined either for the final deuteron or for the final meson. For instance, the deuteron tensor-analyzing power is defined by the cross-section averaged over all spins but the deuteron:

$$T_{20} = \frac{1}{\sqrt{2}} \frac{\sigma(\mathcal{M}_d = 1) + \sigma(\mathcal{M}_d = -1) - 2\sigma(\mathcal{M}_d = 0)}{\sigma(\mathcal{M}_d = 1) + \sigma(\mathcal{M}_d = -1) + \sigma(\mathcal{M}_d = 0)}. \tag{15}$$

It is seen from (15) that in line with the above discussed selection rules, $\sigma(\mathcal{M}_d = 0) \ll \sigma(\mathcal{M}_d = \pm 1)$ and the deuteron tensor-analyzing power is predicted to be almost constant, $T_{20} \approx 1/\sqrt{2}$, in a large region of the energy excess. This prediction is illustrated in fig. 6.

In fig. 7 another polarization observable is depicted defined by

$$W_{zz} = \left. \frac{\sigma(\mathcal{M}_\phi = +1) - \sigma(\mathcal{M}_\phi = -1)}{\sigma(\mathcal{M}_\phi = +1) + \sigma(\mathcal{M}_\phi = -1)} \right|_{s_p = +1/2}, \tag{16}$$

which characterizes the proton-meson spin-spin correlation. As mentioned above, near the threshold the main contribution to $\sigma(\mathcal{M}_\phi = \pm 1)$ comes from the deuteron projections $\mathcal{M}_d = \mp 1$ and, since in (16) the average over the initial neutron polarizations is performed, the quantity W_{zz} is predicted to vanish for the meson exchange diagrams. A substantial deviation of W_{zz} from zero would point to the presence of non-negligible nucleon current contributions in the ϕ production process. In fig. 7 it is seen that there is some weak dependence of W_{zz} upon the energy excess. Nevertheless, W_{zz} remains small indicating that the polarizations of the incident proton and outgoing meson are almost uncorrelated.

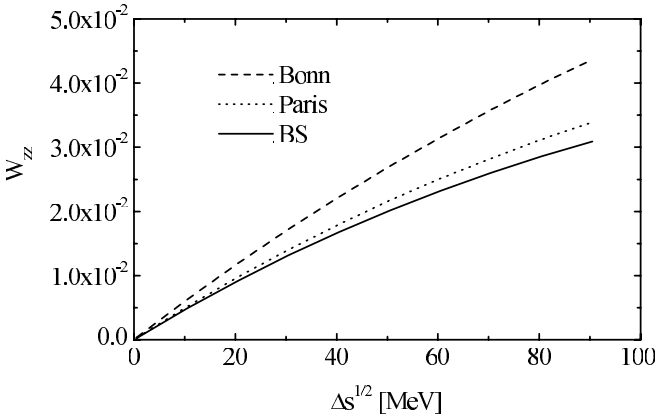

Fig. 7. p-ϕ spin-spin correlation W_{zz} as a function of the excess energy.

A different situation may occur in the reaction $pd \to d\phi p_{\rm sp}$. In this case, if one measures also the polarization of the spectator proton, one may prepare the polarization of the initial deuteron in such a way that the quantity W_{zz} can strongly depend on whether the polarizations of protons are the same or have opposite directions. Let us discuss this assertion in more detail. Adopting for $pd \to d\phi p_{\rm sp}$ the spectator mechanism, as depicted in fig. 8, the invariant amplitude may be expressed through the amplitude of the process $pn \to d\phi$ as follows:

$$\begin{aligned} &\mathcal{F}(s_p, \mathcal{M}_d; s_{p'}, \mathcal{M}_{d'}, \mathcal{M}_\phi) = \\ &\quad \frac{1}{2m} \sum_{s_n} T_{s_p s_n}^{\mathcal{M}_\phi \mathcal{M}_{d'}}(p_p, p_n; p_\phi, p_{d'}) \\ &\quad \times \bar{u}(p_n, s_n)\, \Psi_{\mathcal{M}_d}(n, p')(\widehat{p'} + m) v(p', s_{p'}). \end{aligned} \tag{17}$$

At first glance, since $(\widehat{p'} + m)v(p', s_{p'}) = 0$, the whole amplitude $\mathcal{F}(s_p, \mathcal{M}_d; s_{p'}, \mathcal{M}_{d'}, \mathcal{M}_\phi)$ seems to be zero. This is a usual situation within the BS formalism where one particle (the spectator proton in our case) is on the mass shell. In this case the BS amplitude $\Psi_{\mathcal{M}_d}(n, p')$ itself contains singularities at $p'^2 = m^2$, which exactly compen-

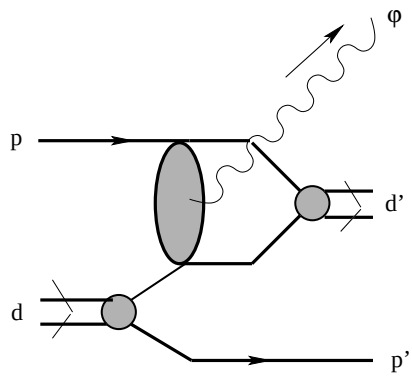

Fig. 8. The diagram for the process $p + d = d' + \phi + p'$ within the spectator mechanism.

sate zeros from inverse propagators, so that the final expression eq. (17) remains finite. Now, from eq. (17) it becomes clear that near the threshold the selection rules for $pd \to d\phi p_{\rm sp}$ reactions are governed by the spin structure of the amplitude $T^{\mathcal{M}_\phi \mathcal{M}_{d'}}_{s_p s_n}(p_p, p_n; p_\phi, p_{d'})$ of the subprocess $pn \to d\phi$. Then, if the spin projection of the initial deuteron $\mathcal{M}_d = 0$, $s_{p'} = 1/2$ implies that the spin of the internal neutron is $s_n = -1/2$. This means that in W_{zz} one has allowed spin transitions as in eq. (16) and, consequently, W_{zz} is predicted to vanish as for the $pn \to d\phi$ reaction. For $s_{p'} = -1/2$ the selection rules predict that, at least in the forward direction, the most probable deuteron final state is that with $\mathcal{M}_{d'} = 0$ and, from helicity conservation, $\mathcal{M}_\phi = 1$. Other spin combinations in the final state are strongly suppressed. Hence, in this case the quantity W_{zz} is expected to be equal to unity in the threshold region.

Since we have $T^{\mathcal{M}_\phi \mathcal{M}_d}_{s_1 s_2}(s,t)$ at our disposal, via eq. (1) any other polarization observable is accessible within our formalism and the corresponding numerical code.

4 Summary

In summary we present here predictions of polarization observables for the quasi-free process $pn \to d\phi$ which are accessible in forthcoming experiments. Off-shell effects in the subprocess $nN \to NN$ can consistently be dealt with, if one restricts the treatment onto the by far dominating meson exchange current. It is the beam target asymmetry which differs drastically from the one in the reaction $pp \to pp\phi$. The tensor-analyzing power is fairly insensitive to variations of the excess energy, and the p-ϕ spin-spin correlation is very small.

Desirable is an extension of the present treatment to incorporate the ω- and ρ-meson production, as done, *e.g.*, in [13] for evaluations of the total cross-section and angular distributions. However, as stressed in [22,23], the elementary amplitude of the $\pi N \to \omega(\rho) N$ subprocess can not be described satisfactorily by one dominating diagram. Rather, a large set of processes including the excitation of baryon resonances in the s-channel contribute to the total cross-section. By virtue of the controversial discussion of the data basis in [24,25] this deserves clarification of the elementary subprocess before one can extend our treatment to other vector mesons, with emphasis to the deuteron in the exit channel.

We are grateful to A.I. Titov for many valuable discussions. The work is supported in parts by BMBF grant 06DR921 and the Landau-Heisenberg program.

References

1. T. Peterson *et al.*, Nucl. Phys. A **663**, 1057c (2000).
2. H. Calén *et al.*, Phys. Rev. Lett. **79**, 2642 (1997), **80**, 2069 (1998), Phys. Rev. C **58**, 2667 (1998); R. Bilger *et al.*, Nucl. Phys. A **663**, 1053c (2000), Nucl. Instrum. Methods A **457**, 64 (2001); P. Moskal *et al.*, Phys. Lett. B **517**, 295 (2001).
3. M. Büscher *et al.*, *Study of ω and ϕ-meson production in the reaction $pd \to dVp_{\rm sp}$ at ANKE*, experiment proposal #75/ANKE, `http://ikpd15.ikp.kfa-juelich.de:8085/doc/Proposals.html`.
4. A. Sibirtsev, W. Cassing, Eur. Phys. J. A **7**, 407 (2000).
5. J. Ellis, M. Karliner, D.E. Kharzeev, M.G. Sapozhnikov, Nucl. Phys. A **673**, 256 (2000).
6. S. von Rotz, M.P. Locher, V.E. Markushin, Eur. Phys. J. A **7**, 261 (2000).
7. J.F. Donoghue, C.R. Nappi, Phys. Lett. B **168**, 105 (1986).
8. J. Gasser, H. Leutwyler, M.E. Sainio, Phys. Lett. B **253**, 252 (1991).
9. J. Ashman *et al.*, Phys. Lett. B **206**, 364 (1988).
10. N. Isgur, H.B. Thacker, Phys. Rev. D **64**, 094507 (2001).
11. T. Schäfer, E.V. Shuryak, hep-lat/0005025
12. L.A. Kondratyuk, Ye. Golubeva, M. Büscher, nucl-th/9808050; V.Yu. Grishina, L.A. Kondratyuk, M. Büscher, Yad. Fiz. **63**, 1923 (2000) nucl-th/9906064.
13. K. Nakayama, J. Haidenbauer, J. Speth, Phys. Rev. C **63**, 015201 (2000).
14. V.Yu. Grishina *et al.*, Phys. Lett. B **475**, 9 (2000), Eur. Phys. J. A **9**, 277 (2000).
15. A.I. Titov, B. Kämpfer, B.L. Reznik, Eur. Phys. J. A **7**, 543 (2000).
16. L.P. Kaptari, B. Kämpfer, S.M. Dorkin, S.S. Semikh, Phys. Rev. C **57**, 1097 (1998); Phys. Lett. B **404**, 8 (1997).
17. L.P. Kaptari, A.Yu. Umnikov, S.G. Bondarenko, K.Yu. Kazakov, F.C. Khanna, B. Kämpfer, Phys. Rev. C **54**, 986 (1996).
18. A.Yu. Umnikov, L.P. Kaptari, F.C. Khanna, Phys. Rev. C **56**, 1700 (1997); A.Yu. Umnikov, L.P. Kaptari, K.Yu. Kazakov, F.C. Khanna, Phys. Lett. B **334**, 163 (1994); A.Yu. Umnikov, Z. Phys. A **357**, 333 (1997).
19. DISTO Collaboration (F. Balestra *et al.*), Phys. Rev. Lett. **81**, 4572 (1998); Phys. Rev. C **63**, 024004 (2001).
20. DISTO Collaboration (F. Balestra *et al.*), Phys. Lett. B **468**, 7 (1999).
21. K. Nakayama, J.W. Durso, J. Haidenbauer, C. Hanhart, Phys. Rev. C **60**, 055209 (1999).
22. B. Friman, M. Lutz, Gy. Wolf, nucl-th/0003012; G. Penner, U. Mosel, Phys. Rev. C **65**, 055202 (2002); M. Post, U. Mosel, Nucl. Phys. A **688**, 808 (2001).
23. A.I. Titov, B. Kämpfer, Eur. Phys. J. A **12**, 217 (2001).
24. C. Hanhart, A. Kudryavtsev, Eur. Phys. J. A **6**, 325 (1999); A. Sibirtsev, W. Cassing, Eur. Phys. J. A **7**, 407 (2000); C. Hanhart, A. Sibirtsev, J. Speth, hep-ph/0107245.
25. G. Penner, U. Mosel, nucl-th/0111024.